Proceedings World Geothermal Congress 2020+1
Reykjavik, Iceland, April - October 2021

Evaluation of cuttings transport impact on percussive drilling performance

Xianfeng Song [1], Gaspar Gohin[2], Trond Bergstrøm[2], Tèrence Coudert[2], and Pascal A. Kane[2, *]

1. Norwegian University of Science and Technology, Trondheim, Norway

2. SINTEF Industry, Trondheim, Norway

Pascal-Alexandre.Kane@sintef.no

Keywords: Geothermal, percussive drilling, cuttings transport, rate of penetration.

ABSTRACT

Down-the-Hole pneumatic percussive tools have demonstrated its high efficiency in completing boreholes in deep hard rock formations, e.g., for harvesting the geothermal energy. Although drilling with such percussive tools has evolved to a mature technology today, fundamental knowledge about the complex process of rock drilling is still lacking, including characterizing the cuttings transport influence on the drilling performance. In this paper, an integrated model is proposed from a hydrodynamic point of view to address the rock cuttings transport and associated critical drilling depth that can be achieved with a Down-The-Hole (DTH) pneumatic hammer for a given pressure delivered by the compressor. Available laboratory data are used to calibrate and validate the multiphase cuttings transport model and hammering dynamics. The results show that the model prediction is able to give a satisfactory accuracy, accounting for the cutting size effect and mass flow influence on the pressure drop. Based on the integrated model, the critical depths for a specified drilling setup are illustrated for various pneumatic pressures.

1. INTRODUCTION

Geothermal energy is recognized as an outperforming renewable energy resource for its tremendous advantages in many aspects, e.g., stable, flexible, and reliable (weather/seasonal independent). Given the fact that the heat is directly extracted from the earth without burning any fossil fuels, such sustainable energy production essentially allows no emissions. Nevertheless, geothermal resources tend to be discovered in deeper and harder geologic formations than typical hydrocarbon reservoirs, which poses considerable restrictions on energy harvesting. (Wittig et al., 2015). Accordingly, enhanced geothermal systems (EGS) is currently seen with great potential for producing significant quantities of geothermal electric power. However, the widespread deployment of EGS is indeed challenged by the high cost of drilling deep wells in the hard rock formations, which requires higher efficiency in hard rock excavation (Song et al., 2019b). In this case, the percussive tools, especially the Down-the-Hole (DTH) percussive tool, has been proved and exploited as a cost/rate-efficient mean for excavating deep medium-hard to extremely hard rock formations (Bjelm, 2006; Cooper et al., 1977; Sheffield and Sitzman, 1985), see Figure 1.

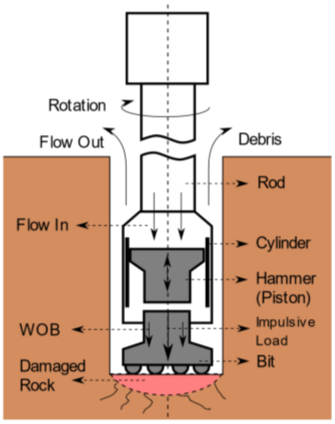

Figure 1: Sketch of DTH drilling (Song et al., 2019a).

Rock excavation in percussive drilling combines crushing, and initiation plus coalescence of tensile side cracks to generate the rock powders and chips, respectively. This effect is achieved from activating an axial reciprocating hammer via pressurized water/air to impact on a continuously rotating drill bit, which then induces (at each impact) compressive stress waves enabling the insert of the hard bit buttons into the rock material. During the penetration process, a sufficient static force, namely weight-on-bit (WOB), is applied on the drill bit to ensure intimate contact between bit and rock for efficient impact transmission. In addition, the superimposed rotary motion allows the drill buttons that positioned in front of the bit with a fixed arc between blows; the subsequent impacts then incline to prompt lateral cracks among craters, namely chipping effects. Rock cuttings are thus formed with lower consumption of impact energy, which can significantly promote the rate of penetration (ROP). Meanwhile, immediate air/water flushing after the impact is necessary to enable efficient rock cuttings removal and expose the fresh rock to the drill bits.

Different types of drilling fluid are used both to drive the machine and transport the rock cuttings during the percussive drilling of a borehole, for instance, the air or the water (Patel, 2019). (Bjelm (2006) claimed that in some applications, the air needs to be replaced with an inert gas to avoid ignition of the hydrocarbon deposit.) Water driven DTH percussive drilling is known for its high output power and blow frequency, greater drilling depth and a dust-free environment, which, however, is limited by the access/storage of water source, onsite water (mud) treatment for hammer systems, and missing water recirculation (Wittig et al., 2015). Instead, pneumatic DTH percussive tool is more flexible for its application of air and longer bit life. Other advantages of applying air in driving the drilling tools include minimization of damage to the boreholes and a higher rate of penetration (Temple, 1999). Although pneumatic percussive tools were introduced about one century ago, fundamental knowledge about the complex process of rock drilling with such tools is still lacking (Song et al., 2019a), including the rock fragmentation and the cuttings transport influence on the deep drilling efficiency.

Several demands need to be fulfilled in order to achieve an optimal drilling condition. Inefficient cuttings transport is recognized that can significantly affect the drilling performance. However, accurate plan and management of the multiphase flow involved in the rock cuttings transport demand ancillary measurement and knowledge, which requires more investigations. It is reported a sudden stall of the borehole assembly was encountered in the well DGE#1 (Lund, Sweden) drilling as a consequence of failure in cleaning the borehole efficiently (Bjelm, 2006). Similar phenomena were also observed by Wittig et al. (2015) and Maurer (1962), where it was claimed inefficient cleaning conditions usually presented in the field drilling and as a result, regrinding of rock cuttings occurred beneath the drill buttons, and the ROP fell below those for perfect cleaning conditions. In contrast, field operations also indicated that excessive airflow to remove the rock cuttings could however induce high economic cost, borehole wash-out, and wear of the system. Therefore, the detailed knowledge of system behavior, especially considering the rock cuttings transport effect, need to be improved given different drilling conditions.

In this paper, an integrated model is proposed from a hydrodynamic point of view to address the rock cuttings transport and associated critical drilling depth that can be achieved with a pneumatic DTH hammer for a given pressure delivered by the compressor. A closed-loop DTH percussive drilling system, reduced to (i) the air compressor, (ii) the pneumatic hammer and (iii) the well annulus, is combined with an empirical ROP law and an analytical multiphase (air, rock cuttings) transport model to predict the drilling performance with depth. Available laboratory data are used to calibrate the multiphase transport model and assess its ability to account for the cutting size distribution and mass flow influence on the pressure drop. In addition, the results from a real-world simulator of a deep well hammer system are used to validate the predicted hammering dynamics. Finally, for illustration purpose, the integrated model is implemented to estimate the critical drilling depth for a specified drilling setup .

2. INTEGRATED MODEL

The pressure distribution along the complete pneumatic DTH percussive drilling system can be considered as an assembly of different segments. In general, the essential subsystems contribute/dissipate the pneumatic pressure in the drilling system include the compressor, the hammer, and the well annulus, schematically shown as Figure 2,

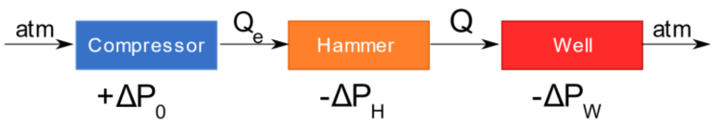

Figure 2: Pressure and flow distribution model.

It is assumed that the working compressor on the ground continuously pumps constant pressure ΔP_0 to the atmospheric airflow to drive the drilling system. For simplicity, leakage of the airflow, e.g., among drill string connectors, is not considered in this study. That is air flux Q_e is conserved until reaching the hammer at the borehole bottom. ΔP_H represents the pressure loss in the hammer, which corresponds to the dissipated energy on percussive activation and ultimate rock fragmentation. The rest of the boosted pressure after the compressor is used to counteract the loss/resistance (ΔP_W) along the borehole annulus that mainly induced by the friction (ΔP_g, either for the fluid or the solid) and the weight of the increasing chips (ΔP_f) with greater borehole depth. In summary, we have the pressure balance for the complete drilling systems:

$$\mathbf{\Delta P_0 = \Delta P_H + \Delta P_W} \tag{1}$$

2.1 Percussive Hammer

DTH percussive drilling is a method where the percussive hammer is positioned at the front of the borehole during drilling, with energy supplied through the drill string in the form of pressurized fluid (Tuomas, 2004). The function of the percussive hammer is thus to convert the high operating pressure into high-shock impact energy for bit penetrations. As the hammer activation within the cylinder occurs so rapidly ($\sim 10^{-2} s$), little energy can be transferred out as heat to the surroundings on this time scale. Therefore, it could be appropriate to assume air decompression in the hammer is an adiabatic process,

$$\frac{\mathbf{Q_e}}{\mathbf{Q}} = \left(\mathbf{1} - \frac{\mathbf{\Delta P_H}}{\mathbf{\Delta P_0 + P_{atm}}}\right)^{\mathbf{1/\gamma}} \tag{2}$$

with the adiabatic index $\gamma = \frac{7}{5}$ for the air and the Q is the subsequent flow rate after activation. Today with the featured bypass choke system, which is popular in the hammer design, DTH hammer allows continuous airflow to stimulate the rock cuttings transport into the borehole annulus. P_{atm} represents the atmospheric pressure. Given the fact that pressure force applied on the drill hammer is usually much larger than its gravity and friction, especially with lubrication, the hammer movement is thus assumed to be only driven by the pressure force when evaluating hammer dynamics. From the mechanical point of view, the hammer is then accelerated linearly along the hammer cylinder, see Figure 3. Accordingly, the hammer impact velocity v_i can be determined as

$$v_i = 2\delta f \qquad (3)$$

where δ refers to the hammer stroke and f is the hammering frequency. For simplicity, the control valve is not considered in this study, which will affect the consecutive impacts in multi-impact analyses.

In this case, each impact energy of the drill hammer is $E_i = 2m_p\delta^2 f^2$, where m_p is the hammer mass. Correspondingly, the impact power of the hammer is thus $\mathcal{P}_{\mathcal{H}} = f_i E_i$, and $f_i = \frac{f}{2}$ is the impact frequency since the hammer hits sequentially the cylinder bottom and top during one cycle. Meanwhile, from the aerodynamic point of view, the consumed power on impact drill bit can also be represented by $\mathcal{P}_{\mathcal{H}} = \Delta P_H Q_e/2$, which leads to the fundamental laws of the hammer operation:

$$\Delta P_H = \frac{2m_p}{\delta s^3} Q_e^2 \qquad (4)$$

$$f = \frac{Q_e}{V_p} \qquad (5)$$

$$E_i = V_p \Delta P_H \qquad (6)$$

where the chamber in the cylinder for hammer acceleration is assumed to be uniform with cross-sectional area s. Thus, the chamber volume is $V_p = s\delta$.

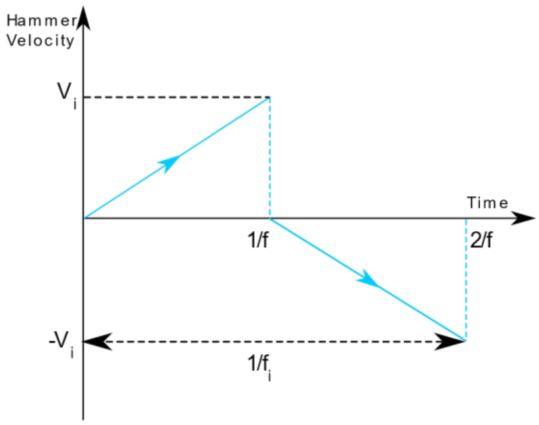

Figure 3: Hammer linearly accelerates as a function of time (period movement).

2.2 Empirical ROP Prediction

An efficient rock penetration process is essential for drilling overall competitiveness and productivity (Tuomas, 2004). It is observed the ROP for the percussive drilling methods depends primarily on (i) machine designs, i.e., hammer and bit types, bit button numbers, positions and shapes, flushing hole positions and sizes, etc.; (ii) operational variables, such as indexing angles (relies on the rotation speed and impact frequency), weight-on-bit, pneumatic feed pressure, impact energy/frequency, and flushing efficiency; (iii) the rock properties (Tuomas, 2004). To achieve an accurate prediction of ROP, one obvious way of overcoming these uncertainties is thus to average many indentations rather than get an accurate estimation of every single impact (Hustrulid and Fairhurst, 1971). A review of the experimental evidence indeed reflected a linear relationship between dissipated energy and crater volumes (Song et al., 2019b). That is the specific energy E_s, defined as the energy required to remove a unit volume of rock, characterizing the rock drillability essentially remains the same under otherwise constant conditions.

During the hammer activation process, the impact of the hammer on the rest drill bit provokes an impulsive load that can enable the insert of bit buttons into the rock materials. Consider the gap of the timescale between the hammer impact ($\sim 10^{-2}s$) and stress wave transmission ($\sim 10^{-4}s$), this bit penetration process is assumed to be accomplished instantaneously. However, the rock, while dissipating most of the impact energy on rock fragmentation (assume all the energy absorbed by the rock is used for crush work), will also simultaneously reflect a certain amount of energy and distribute it among the drilling components (Chiang and Elias, 2000). In other words, a total of ηE_i out of the impact energy can be transferred and ultimately dissipated on rock fragmentation, where coefficient η represents the energy transfer efficiency. Furthermore, it was claimed the time interval between impacts is long enough for the rest of the energy stored in the drilling components to fade out (Lundberg, 1971). Therefore, consecutive hammer impacts can be treated to be independent. This can also be revealed from the repetitiveness among successive blows in percussive drilling demonstrated by Hustrulid (1965) and Hartman (1966). In all cases, the recorded impacts and crater volumes are nearly the same given the same drilling conditions. Therefore, the averaged ROP can be evaluated as:

$$Rop = f_i \frac{\eta E_i}{A E_s} \qquad (7)$$

where A is the borehole cross-sectional area (Hustrulid and Fairhurst, 1972). Consider the rock cuttings mass conservation during the efficient pneumatic transport, the solid mass flow rate $\dot{m}$ can be determined as:

$$\dot{m} = A\rho_s Rop \qquad (8)$$

where ρ_s is the rock density.

2.3 Multiphase Flow

It is known a fraction of energy carried by the compressed air is spent on fragmenting the rock, while the rest is dedicated to transporting the rock cuttings out of the borehole. In fact, in the view of the stationary airflow in the vertical borehole annulus, consider one spherical rock particle with diameter d that is injected from the rock formation after excavation and been transported in the annulus, its gravity W_s should be balanced by the turbulent drag force F_d induced by the airflow (with density of ρ_g):

$$W_s = \frac{\pi}{6}\rho_s g d^3 \tag{9}$$

$$F_d = \frac{1}{2}\rho_g C_d A_s v_t^2 \tag{10}$$

where g is the gravitational acceleration, $A_s = \frac{\pi d^2}{4}$ is the cross-sectional area of the spherical rock particle, and v_t is the slip velocity (settling velocity) between the rock cuttings and airflow. Therefore, the slip velocity can be determined as: $v_t = \sqrt{\frac{4gd\rho_s}{3C_d\rho_g}}$. The particle velocity can be estimated with higher accuracy if the interaction among rock cuttings is taken into account. Levy (2000) claimed that for the cuttings transport where the solid concentration ε less than 0.2, as investigated in this study ($\varepsilon \sim 10^{-3}$, which is affected by the actual flow rate, ROP, and the density of the drilled rock), the slip velocity can be empirically evaluated as:

$$v_t' = v_t(1-\varepsilon)^{0.825} \tag{11}$$

Therefore, in this case, it is accurate enough to use v_t to approximate v_t'. And the drag coefficient C_d can be determined by:

$$C_d = \max\left\{\frac{24}{R_e}(1+0.15R_e^{0.687}), 0.44\right\} \tag{12}$$

where the particle Reynolds number is:

$$R_e = \frac{\rho_g d(1-\varepsilon)v_t'}{\mu} \tag{13}$$

and μ is the dynamic viscosity (Levy, 2000). Indeed, the pressure loss due to friction essentially has two sources: the fluid-wall friction (ΔP_{f_f}) and the solids-wall friction (ΔP_{f_s}). In the first case, the Darcy-Weisbach equation was proposed to evaluate the fluid frictional loss:

$$\Delta P_{f_f} = L(1-\varepsilon)f_D \frac{\rho_g}{2}\frac{v_g^2}{D_h} \tag{15}$$

where f_D is the Darcy coefficient, and D_h is the hydraulic diameter defined as the error between the borehole diameter D_o and the drill string diameter D_i. Several relations exist to compute this coefficient. In this study, the Blasius relation is adopted as it is valid for Reynolds number up to 10^5:

$$f_D = 0.316R_e^{-\frac{1}{4}} \tag{16}$$

Similarly, in terms of estimating particles-wall friction, the pressure loss can be expressed as follows:

$$\Delta P_{f_s} = L\varepsilon f_s \frac{\rho_s}{2}\frac{v_s^2}{D_h} \tag{17}$$

where L is the length/depth of the borehole, f_s is the solids friction coefficient and $v_s = v_g - v_t$ is the cuttings transport velocity. In this case, many empirical expressions have been proposed to represent the coefficient f_s (Rajan, 2012). It happens that none of the introduced empirical expressions can comprehensively match the experimental results given below. In order to take the joint influence from the particle fraction ε, the particles diameter d, and the solids speed v_s into account, the following general expression is proposed to represent f_s:

$$f_s = a_0\varepsilon^{a_1}d^{a_2}v_s^{a_3} \tag{18}$$

with (a_0, a_1, a_2, a_3) are unknown coefficients to be determined by matching with the experimental data.

In addition, solid concentrations during cuttings transport induce extra pressure loss along the borehole annulus. The pressure loss ΔP_g due to the accumulated weight of particles and air in the borehole annulus can be simply given by the relation:

$$\Delta P_g = Lg(\varepsilon\rho_s + (1-\varepsilon)\rho_g) \tag{14}$$

To sum up, the total pressure loss in the well can be expressed as:

$$\Delta P_w = L\left[\varepsilon\rho_s\left(g + \frac{f_s}{2}\frac{v_s^2}{D_h}\right) + (1-\varepsilon)\rho_g\left(g + \frac{f_D}{2}\frac{v_g^2}{D_h}\right)\right] \tag{19}$$

2.4 Dimensionless Analysis

In order to reduce the number of parameters when processing the whole system dynamics, it is rather convenient to reformulate the aforementioned equations in a dimensionless form by introducing scales. In this case, the condition at borehole length equals to zero can be referred to as the benchmark to calibrate and understand the influence of different factors on the drilling performance. Accordingly, the impact from the well pressure drop is eliminated, which implies that $\mathbf{\Delta P_0 = \Delta P_H}$. Therefore, the complete system can be expressed in the dimensionless form:

$$\begin{cases} q_e = \frac{Q_e}{Q_{e,0}} \\ q = \frac{Q}{Q_0} \\ p_H = \frac{\Delta P_H}{\Delta P_0} \\ p_W = \frac{\Delta P_W}{\Delta P_0} \\ rop = \frac{Rop}{Rop_0} \end{cases} \rightarrow \begin{cases} p_W + p_H = 1 \\ q_e = \sqrt{p_H} \\ q = \left(\frac{1-\alpha}{1-\alpha p_H}\right)^{\frac{1}{\gamma}} \sqrt{p_H} \\ rop = p_H^{\frac{3}{2}} \\ l = (1 - p_H) / \left(q^2 + \beta \frac{p_H^3}{\varepsilon} + p_g\right) \end{cases} \tag{20}$$

where parameters with subscript 0 correspond to the value evaluated at borehole depth equals to zero. And with the dimensionless parameters:

$$\begin{cases} l = \frac{L}{L_f} \\ \alpha = \frac{\Delta P_0}{\Delta P_0 + P_{atm}} \\ \beta = \frac{L_f}{L_s} \\ p_g = \frac{L_f g(\rho_g + \varepsilon \rho_s)}{\Delta P_0} \end{cases} \tag{21}$$

as well as the characteristic length:

$$\begin{cases} L_f = \frac{2 D_h S^2 \Delta P_0}{f_D \rho_g Q_0^2} \\ L_s = \frac{2 \rho_s D_h S^2 \Delta P_0}{f_s \dot{m}_0} \end{cases} \tag{22}$$

where $S = \frac{D_o^2 - D_i^2}{4}$ is the area of the borehole annulus.

3. Model Analysis

The pneumatic DTH percussive drilling tools have been widely used in mining and geothermal industry. The available data from a real-world simulator of a hammer for deep hole drilling (Halco Dominator 880 Deep Well) are used as the 'experimental' observations for calibrating and comparing with the predicted hammering dynamics, where the hammer specifications are: hammer mass $m_p = 43.63\ kg$, hammer stroke $\delta = 0.125\ m$ and hammer section area $s = 0.0144\ m^2$.

In general, according to the results illustrated in Figure 4, it can be concluded that the predicted results of the airflow and the impact frequency are able to fit the data with acceptable accuracy. However, in terms of the estimated hammer impact velocity, impact energy and impact power, a significant discrepancy can be observed between the model and the data. The model produces up to two times larger prediction than the data under higher air-driven pressures. This can partially be attributed to the fact that the friction effect is neglected in the model, and the valve for controlling the airflow is not considered either.

In terms of validating the rock cuttings transport model, it is noticed that Temple (1999) performed a series of laboratory-scale experiments to investigate the pressure loss in pneumatic solids transport. In this attempt, dry air was utilized as the circulating flow medium. The aim of this experimental study is to characterize the evolution of pressure loss ΔP_w as a function of the air velocity v_g at various solid sizes and mass flow rates. Sintered bauxite spheres were used in the experiments ($\rho_s \sim 3100\ kg/m^3$, approximate rock cuttings) to minimize the impact from particle attrition (change of particle size). They were injected at the base of the apparatus with a predominated flow rate controlled by a valve. A general evolution tendency was captured, see Figure 5, where it was found the airflow requires a minimum velocity, defined as the 'choking' velocity, to lift the particles. This critical value is speculated to essentially correspond to the slip velocity v_t evaluated in this study. In this case, if the pneumatic driven velocity v_g is below the choking velocity, then the particles deposit and interact with each other, so gravitational effects on the particles predominate. Consequently, it forms slugs, causes vibrations of the drill pipe, and significant pressure drops. Interestingly, it was found as the annular air velocities were increased, an optimal airflow velocity emerged, which can be exploited to minimize the pressure drops. However, the plot also indicates that as the air velocity was further increased (greater than the optimal velocity), then the pressure drops increase as the frictional pressure losses predominate (Temple, 1999).

From Figure 6, it can be seen that this non-monotonical pressure drops characteristic is accurately captured by the proposed model. In particular, given the definite particle size ($346.5\ \mu m$), several mass flow rates were tested, and it was observed that the optimal air velocities were essentially the same for different mass flow rate. And this effect of minimum pressure drop depends primarily on particle sizes, and to a little degree on the solid flow rate, is also revealed by the model with relatively high accuracy, see the comparison between the model predicted pressure loss and the experimental measurement in Figure 6. In addition, it is noticed that the minimum pressure drops increase with solid flow rates. This behavior is expected as the friction and viscosity increase with the number of solids present in the multiphase flow.

Similarly, particle sizes effect was investigated by considering three different particle diameters under the same flow rate ($25\ g/s$), see Figure 7. The results indicate that the minimum pressure drops increase with the particle sizes since a larger slip velocity/air velocity is required in order to produce sufficient drag force to carry the solid particles. The effect of friction on the annulus walls is thus more pronounced.

As can be seen in Figure 6 and Figure 7, an important limiting factor during downward vertical/inclined borehole drilling is the speed of the flushing media (Tuomas, 2004). That is the air velocity is required to be larger than the slip velocity in order to lift the rock particles: $v_g > v_t$,. Therefore, it reveals the presence of a critical drilling depth for a given pneumatic pressure, since the pressure loss along with the borehole annulus increases with drilling depth. A numerical solution is then obtained for resolving the evolution of a set of non-dimensional drilling variables as a function of increasing drilling depth, see Figure 8~10Figure 4. For illustration purpose, the chosen drilling parameters are given in Table 1. Besides, it was denoted particle size distribution in percussive drilling varies with many factors, such as the rock properties, drill bit design, indexing angle and impact energy (Tuomas, 2004). In this case, the spheric particle diameter is assumed to be fixed ($5mm$). The induced critical depth given such drilling condition is presented in Figure 11.

The prediction results imply the critical depth increases with the capacity of the compressor, which is in agreement with the observations in actual drilling. In particular, the obtained values for the critical depth essentially correspond with the usual drilling depth reached in practice (without booster). Therefore, it could explain the physical limitation of drilling depth from a hydrodynamic point of view that observed in pneumatic DTH percussive drilling.

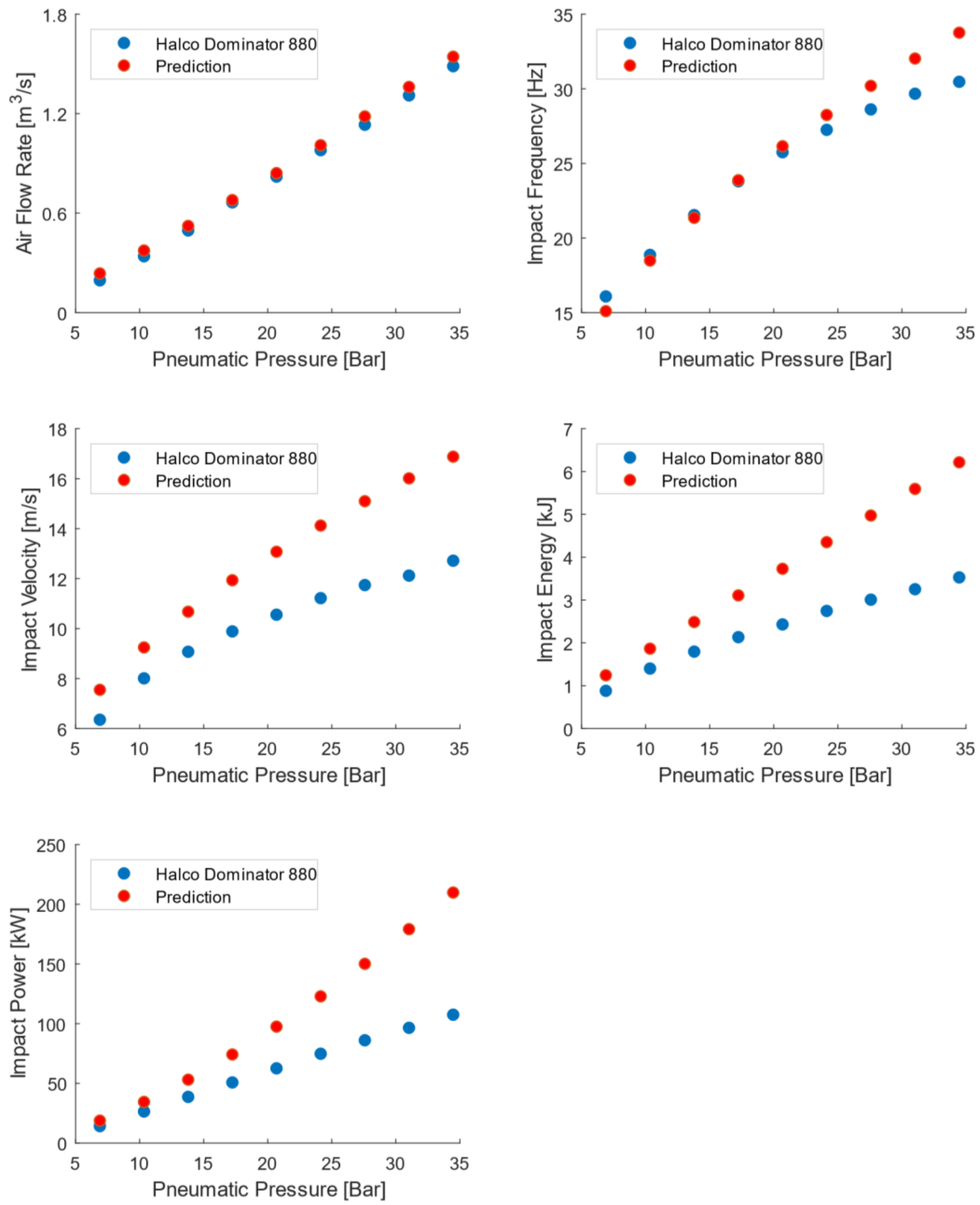

Figure 4: Comparison between the predicted and 'experimental' hammer performance.

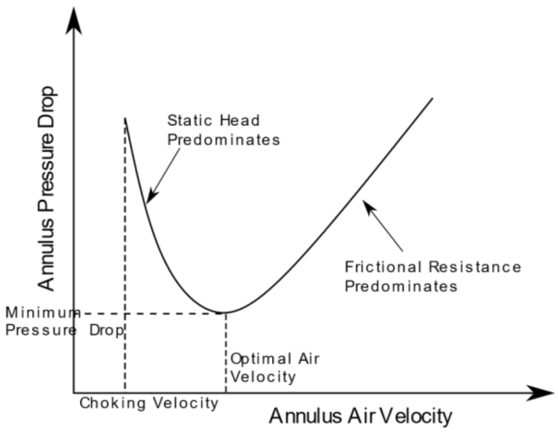

Figure 5: Pressure drop versus annular air velocity for an air-solids system (Temple, 1999).

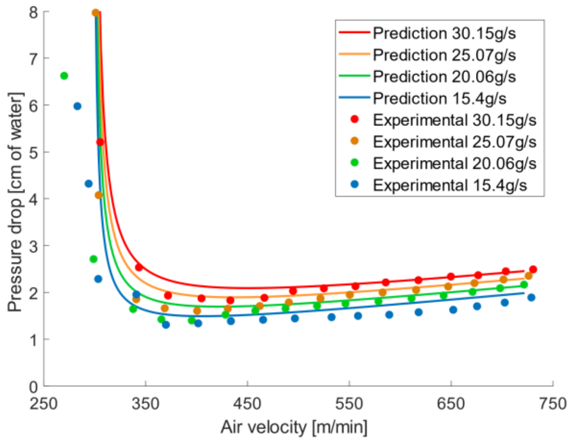

Figure 6: Comparison between the theoretical and experimental results of the pressure drops vs. air velocity for different mass flow rates.

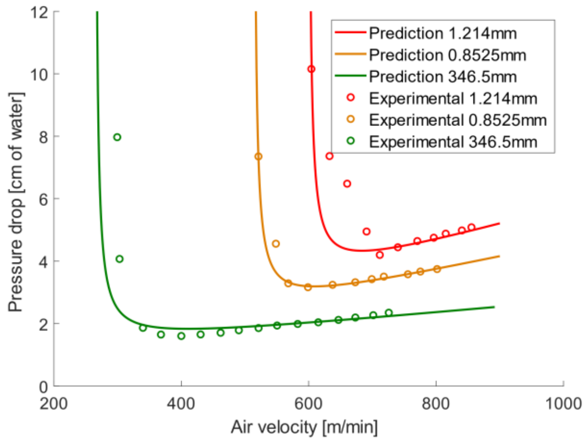

Figure 7: Comparison between the theoretical and experimental results of the pressure drops vs. air velocity for different particle sizes.

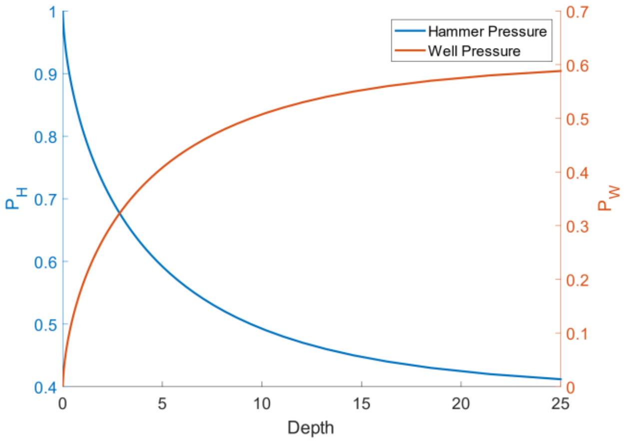

Figure 8: Dimensionless pressure distribution with increasing drilling depth.

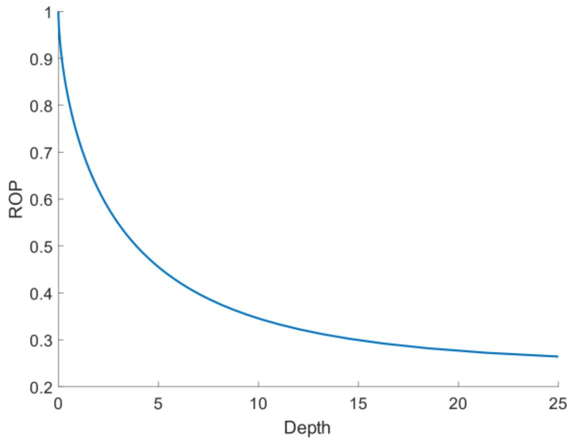

Figure 9: Decreasing ROP with increasing drilling depth.

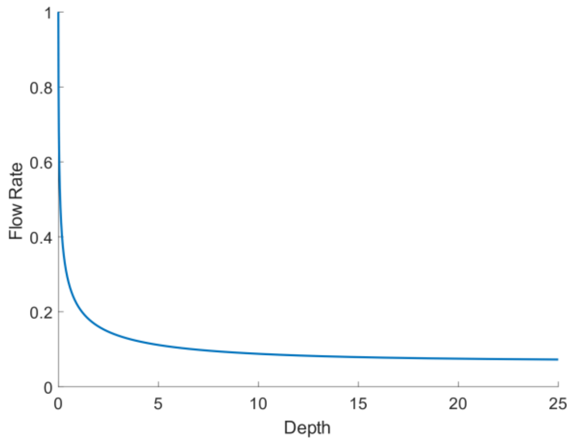

Figure 10: Decreasing flow rate with increasing drilling depth.

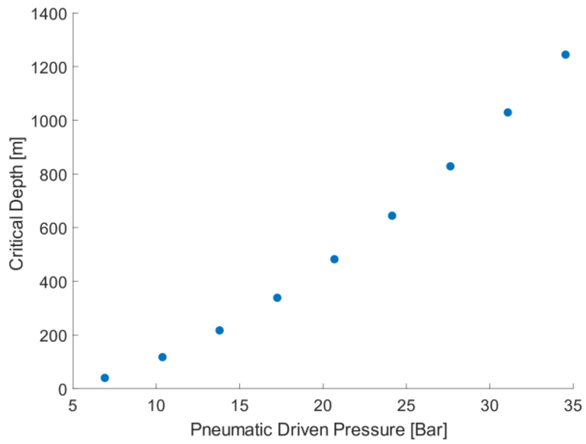

Figure 11: Influence of pneumatic driven pressure on the critical drilling depth.

Table 1: Parameters used for prediction.

Rock Density ρ_s	2750 kg/m^3	Air Density ρ_g	1.225 kg/m^3
Outer Diameter D_o	0.2 m	Inner Diameter D_i	0.18 m
Rop_0	10 m/h	Pneumatic Pressure ΔP_0	34.5 Bar

4. DISCUSSIONS

In this paper, an integrated model is proposed from a hydrodynamic point of view to investigate the rock cuttings transport impact on the percussive drilling performance. A closed-loop DTH percussive drilling system, reduced to (i) the air compressor, (ii) the pneumatic hammer and (iii) the well annulus, is combined with an empirical ROP law and an analytical multiphase (air, rock cuttings) transport model to predict the pressure loss and associated drilling variables evolution with increasing depth. Available laboratory data are used to calibrate the multiphase transport model and assess its ability to account for the cutting size distribution and mass flow influence on the pressure drop. The critical depths predicted by the integrated model are illustrated for various compressor capacity. The obtained values correspond well with the outcome usually observed during the actual drilling process. However, in practice, rock cuttings with large size potentially never reach to the surface due to the limited airflow rates. Hence, these rock cuttings fall back down the annulus and to be reground by the bits into small particles until their sizes are small enough to be flushed. In this case, the penetration rate is reduced, and the actual rock cuttings transport condition becomes significantly sophisticated. And free water can add additional flowing phase in the cuttings transport, especially for harvesting conventional hydrothermal resources and need further investigations.

ACKNOWLEDGMENT

This study is a part of the research project INNO-Drill (Technology platform for research-based innovations in deep geothermal drilling) funded by The Research Council of Norway (grant 254984) and industry partners (Epiroc, Enel Green Power, Lyng Drilling, NOV, Ravel, Robit, Rock Energy, Sandvik Mining and Construction, Tomax and Zaptec).

REFERENCES

Bjelm, L.: Under Balanced Drilling and Possible Well Bore Damage in Low Temperature Geothermal Environments, *Proceedings*, 31st Workshop on Geothermal Reservoir Engineering, Stanford University, Stanford, CA (2006).

Cooper, L.W.: Hook, R.A., and Payne, B.R.: Air Drilling Techniques, *Proceedings*, Deep Drilling and Production Symposium of the Society of Petroleum Engineers of AIME, Amarillo, TX (1977).

Chiang, L. E. and D. A. Elias.: Modeling impact in down-the-hole rock drilling, *Article*, International Journal of Rock Mechanics and Mining Sciences. 37(4): 599-613 (2000).

Hartman, H. L.: The Effectiveness of Indexing in Percussion and Rotary Drilling, *Article*, International Journal of Rock Mechanics & Mining Sciences, 3:265–278 (1966).

Hustrulid, W. A.: A Study of Energy Transfer to Rock and Prediction of Drilling Rates in Percussive Drilling, *Master Thesis*, University of Minnesota (1965).

Hustrulid, W. A. and Fairhurst, C.: A theoretical and experimental study of the percussive drilling of rock Part II-force-penetration and specific energy determinations, *Article*, International Journal of Rock Mechanics and Mining Sciences & Geomechanics Abstracts, 8 (4): 335-356 (1971).

Hustrulid, W. A. and Fairhurst, C.: A theoretical and experimental study of the percussive drilling of rock Part IV-application of the model to actual percussion drilling, *Article*, International Journal of Rock Mechanics and Mining Sciences & Geomechanics Abstracts, 9 (3): 431-442 (1972).

Lundberg, B.: Some basic problems in percussive rock destruction, Ph.D. Thesis, Chalmers University of Technology, Sweden (1971).

Maurer, W.C.: The “Perfect -Cleaning” Theory of Rotary Drilling, *Proceedings*, 37th Annual Fall Meeting of SPE, Los Angeles, CA (1962).

Patel, A.: Geotechnical investigation, *Book*, Geotechnical Investigations and Improvement of Ground Conditions, A volume in Woodhead Publishing Series in Civil and Structural Engineering (2019).

Rajan, K.S.: Simulation Of Vertical Gas-Solid Flow: Comparison of Correlations for Particle-Wall Friction and Drag Coefficient, *article*, International Journal of ChemTech Research, Vol.4, No.4, pp 1314-1321 (2012).

Sheffield, J.S., and Sitzman, J.J.: Air Drilling Practices in the Mid-continent and Rocky Mountain Areas, Proceedings, SPE/IADC Drilling Conference, New Orleans, LA (1985).

Song, X., Kane, P.A., Aamo, O.M., and Detournay, E.: A dynamic model of the drilling action of percussive tools, *Proceedings*, 53rd US Rock Mechanics/Geomechanics Symposium, NewYork, NY (2019a).

Song, X., Aamo, O.M., Kane, P.A., and Detournay, E.: A Phenomenological Model of Percussive Drilling: Review of Experimental Evidence, *Proceedings,* ARMA-CUPB Geothermal International Conference, Beijing, CN (2019b).

Tuomas, G.: Water powered percussive rock drilling, *Ph.D. Thesis*, Luleå University of Technology, Sweden (2004).

Wittig, V., Bracke, R., and Ick, Y.H.: Hydraulic DTH Fluid / Mud Hammers with Recirculation Capabilities to Improve ROP and Hole Cleaning For Deep, Hard Rock Geothermal Drilling, *Proceedings*, World Geothermal Congress, Melbourne, Australia (2015).